DOI: 10.1002/ejic.200601036

Copper(II)–Purine Complexes Encapsulated in NaY Zeolite

Natércia Nunes,[a] Raquel Amaro,[a] Filomena Costa,[a] Elisabetta Rombi,[b] M. Alice Carvalho,[a] Isabel C. Neves,*[a] and António M. Fonseca[a]

Keywords: N ligands / Copper / NaY / Encapsulation / Host–guest chemistry / Oxidation

Y-encapsulated Cu^{II}–purine complexes were synthesized, characterized and studied in the catalytic oxidation of cyclohexene. Encapsulation was achieved by ion-exchanging the complex from aqueous solutions containing both the purine ligand, 9-methyl-6-(methylamino)purine, and copper, in different pH, with a purine/Cu^{II} molar ratio of 5:1. The resulting materials were characterized by surface analysis (XPS, SEM and XRD), chemical analysis, spectroscopic methods (EPR, FTIR and UV/Vis) and thermal analysis (TGA), which indicated that the Cu^{II}–purine complexes were effectively encapsulated in NaY, most probably inside the supercages, without any modification of the morphology and structure of the zeolite. Different Cu^{II}–purine complexes were formed, depending on the pH during synthesis. The coordination geometry of Y-encapsulated Cu^{II}–purine complexes was obtained with preferentially 1:2 and 1:3 Cu/L stoichiometry: complexes **A** and **B** (1:2) and complex **C** (1:3). Complex **A** was formed at pH ≥ 7, and complexes **B** and **C** (Scheme 2) were formed at pH = 5.4. Oxidation of cyclohexene with *t*BuOOH (TBHP) as the oxygen source, gave 2-cyclohexene-1-one, 2-cyclohexene-1-ol, cyclohexene oxide and 3-*tert*-butylcyclohexenyl peroxide.

Introduction

During the last two decades the preparation and catalytic activity of transition-metal complexes encapsulated in zeolite structures have been extensively investigated because of their industrial significance. The use of metal complexes immobilized into solid supports as heterogeneous catalysts has become very important for ecofriendly industrial processes. These new catalysts can be easily separated from the reaction mixture and which also improves the recycling of the expensive catalyst.[1,2]

Encapsulation of transition-metal complexes with redox properties, in zeolites or other molecular sieves, is a theme of current research because of their potential use as heterogeneous redox catalysts. The peculiar adsorptive properties of Y zeolites originate from the positively charged exchangeable ions, which are located inside the 3D pore structure of the solid to balance the negative charge on the framework Al atoms and which can be coordinated by different functionalized ligands.[3]

The oxyfunctionalization of inexpensive hydrocarbons to produce more valuable organic compounds, such as alcohols, aldehydes and ketones, requires the selective oxidation of strong C–H bonds.[4,5] In this field, homogeneous catalysis is not suitable for applications on a large scale, because of low conversions, catalyst deactivation, the cost of the complexes and lack of recycling methods.

Y-encapsulated Cu^{II}–histidine complexes showed good catalytic activity in the oxidation of alcohols and alkenes in the presence of hydrogen peroxide at ambient temperatures.[6–10] Alkene oxidation led to different products, depending on the structure of both the substrate and the oxidant.[11] Heterogenized copper(II)–amino-acid complexes $[Cu(AA)_n]^{m+}$ were obtained by Weckhuysen et al.[6] by encapsulation in Y zeolites through ion exchange from aqueous solutions containing both the amino acid (AA) and copper(II), with an AA/Cu^{II} ratio of 5:1. Copper(II) was chosen as the transition-metal ion because it forms the most stable coordination complexes, which typically consist of four nearby donor atoms approximately arranged in a plane around the transition-metal ion.[6–8]

The present work deals with the multistep preparation, characterization and catalytic studies of new heterogeneous materials, namely Cu^{II}–purine complexes encapsulated in Y zeolites. The preparation procedure includes (i) the synthesis of purine ligands and (ii) the ion-exchange procedure for encapsulating the metal complex in the NaY zeolite. The obtained samples were fully characterized by chemical analysis, spectroscopic methods (EPR, FTIR and UV/Vis), powder X-ray diffraction (XRD), X-ray photoelectron spectroscopy (XPS), scanning electron microscopy (SEM) and thermal analysis (TGA). The cyclohexene oxidation reaction was performed in liquid phase, at 30 °C, by using *tert*-butyl hydroperoxide (*t*BuOOH) as the oxygen source.

[a] Departamento de Química, Centro de Química, Universidade do Minho,
Campus de Gualtar, 4710-057 Braga, Portugal
Fax: +351-253-678983
E-mail: ineves@quimica.uminho.pt
[b] Dipartimento di Scienze Chimiche, Università di Cagliari, Monserrato, Italy

Results and Discussion

The 9-Methyl-6-(methylamino)purine Ligand

The biomonomer under investigation, 9-methyl-6-(methylamino)purine, a potentially polydentate ligand, can offer only nitrogen atoms as donor atoms. It was suggested that the most basic centre in purine resides in the pyrimidine ring, especially at N^1. However, protonation can also occur at N^7 and N^9.[12]

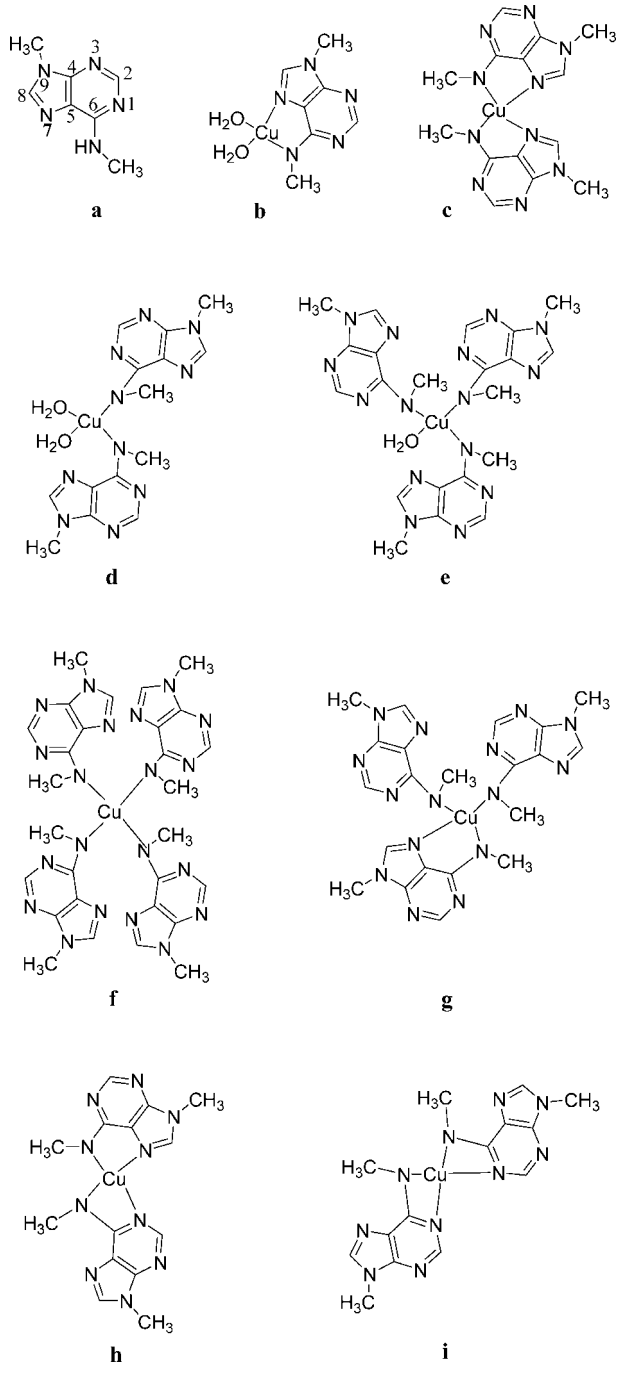

Scheme 1. Molecular structures of the used ligand and possible models of purine coordination in copper complexes: **a**: 9-methyl-6-(methylamino)purine; **b**: $N_{am}N^7O_wO_w$; **c**: $N_{am}(1)N^7(1)N_{am}(2)N^7(2)$; **d**: $N_{am}(1)N_{am}(2)O_wO_w$; **e**: $N_{am}(1)N_{am}(2)N_{am}(3)O_w$; **f**: $N_{am}(1)$-$N_{am}(2)N_{am}(3)N_{am}(4)$; **g**: $N_{am}(1)N_{am}(2)N_{am}(3)N^7(3)$; **h**: $N_{am}(1)$-$N^7(1)N_{am}(2)N^1(2)$; and **i**: $N_{am}(1)N^1(1)N_{am}(2)N^1(2)$ coordination. The axial ligands are omitted in these representations.

Since N^9 is substituted in the 9-methyl-6-(methylamino)-purine ligand, the coordination of the ligand with the copper ion can occur at N^1 and N^7 on the purine ring and at the *N*-amino nitrogen (N_{am}), which is bonded to C^6 carbon of the six-membered ring. Accordingly, different models of purine coordination in copper complexes can be derived (Scheme 1).

As shown in Scheme 1, the purine ligand can coordinate with the copper ion to generate complexes with four- and five-membered chelating rings; however, the latter ones lead to minor ring tension and to less steric hindrance, being thus preferred.

The purine ligand was characterized by spectroscopic methods. The electronic absorption spectrum of the purine ligand for pH = 7.0 and 10.0 exhibits three slight bands at λ_{max}(EtOH) = 305, 320 and 335 nm, which can be assigned to ligand n-π* transitions, and a high intense broad band at λ_{max}(EtOH) = 269 nm due to π-π* transitions.[13,14] A similar spectrum was obtained for pH = 5.4, however, a small shift to higher transition energies due to N^1 nitrogen protonation was observed.

The FTIR spectrum of the ligand in KBr is dominated by the characteristic bands of the purine ring ($\tilde{\nu}_{max}$ = 1617–1300 cm^{-1}) and by bands of the methylamino group on the 6-position of the ring ($\tilde{\nu}_{max}$ = 3273 and 1679 cm^{-1}). The strong and medium bands appearing between $\tilde{\nu}_{max}$ = 1617 and 1300 cm^{-1} can be attributed to skeletal vibrations of the purine ring, while the methylamino group is indicated by the typical free N–H stretching vibrations at $\tilde{\nu}_{max}$ = 3273 cm^{-1} and by the N–H bending vibration at $\tilde{\nu}_{max}$ = 1679 cm^{-1}.[13]

Ion-Exchange Encapsulation Process of Cu^{II}–Purine Complexes

As it is commonly known, NaY zeolite is a microporous aluminosilicate based on sodalite cages joined by O bridges between the hexagonal faces. Eight such sodalite cages are linked together, forming a large central cavity or supercage, with a diameter of 12.5 Å. The supercages share a 12-membered ring with an open diameter of 7.4 Å. Thus, Cu^{II}–purine complexes can be ion-exchanged and encapsulated into the zeolite cavities.[15] In earlier studies, we showed that the methodologies used for the encapsulation/immobilization of the metal complexes in zeolites[16] and clays[17] are largely determined by the supports.

In this work, the modified zeolites with the entrapped metal complex were prepared by ion exchange in aqueous solutions, using an excess of the purine ligand (purine/Cu^{II} molar ratio = 5:1). Chemical analysis (ICP-AES), and FTIR and UV/Vis spectroscopic analyses were performed at different stages of the preparation procedure in order to better characterize the prepared materials. In particular, the residual solutions obtained from the encapsulation process

were analyzed before and after Soxhlet extraction. The results are summarized in Table 1.

Table 1. Chemical analysis of the residual solutions after the ion-exchange procedure for the preparation of the $[Cu^{II}L]_nY$ samples.

Sample	Cu^{II} [a] [mmol]	Cu^{II} [b] [mmol]	Cu^{II} [c] [mmol]	Cu^{II} [d] [mmol]
$[Cu^{II}L]_{5.4}Y$	3.52×10^{-2}	1.65×10^{-5}	3.518×10^{-2}	–
$[Cu^{II}L]_7Y$	3.52×10^{-2}	3.15×10^{-5}	3.517×10^{-2}	3.38×10^{-2}
$[Cu^{II}L]_{10}Y$	3.52×10^{-2}	1.57×10^{-5}	3.518×10^{-2}	–

[a] Initial copper amount in the ion-exchange solution. [b] Residual copper amount. [c] Copper loading on NaY. [d] Copper loading on NaY after the treatment with $NaNO_3$.

It appears that the residual Cu^{II} content was very low, indicating that about 99% of the copper initially present was retained inside the zeolite. This finding was also confirmed by the disappearance of the brown-green colour of the starting solution after six hours under ion exchange with the zeolite.

For the sample of $[Cu^{II}L]_7Y$ submitted to the treatment with $NaNO_3$, the amount of uncomplexed copper ions in solution was equal to 1.40×10^{-3} mmol, implying a copper loading on NaY of 3.38×10^{-2} mmol. The small decrease observed in the loaded amount of Cu^{II}, on the $[Cu^{II}L]_7Y$ sample after the $NaNO_3$ treatment, seems to indicate that almost all the adsorbed metal (96%) reacted with the purine ligand and the resulting complex became entrapped inside the zeolite.

$[Cu^{II}L]_nY$ before Soxhlet Extraction

To obtain information about the adsorption of the purine ligand on zeolite, the residual solutions of the ion-exchange procedure were further analyzed by UV/Vis and FTIR spectroscopy. The presence of the purine ligand in the residual solutions is shown by the appearance of the band at λ_{max}(EtOH) = 269 nm in the UV/Vis spectra, thus indicating that the excess ligand in the initial solutions, not adsorbed by zeolite, was removed by filtration. The IR measurements also reveal the presence of bands due to the ligand, thus confirming the UV/Vis spectra results.

$[Cu^{II}L]_nY$ after Soxhlet Extraction

Zeolites with the hosted metal complex, which were a brown-green colour, were extracted with ethanol to remove both the residual metal complex physically adsorbed on the external surface and the uncomplexed ligand. The resulting samples retained their initial colour after extraction. FTIR and UV/Vis spectroscopic analyses were performed on the extracting solvent; typical absorption bands of the purine ligand and complexes were present in the obtained spectra. These results confirmed that Soxhlet extraction was able to remove the entire adsorbed complex on the external surface and the uncomplexed ligand. This finding might indicate that the adsorbed ligand is fully coordinated with copper ions and that the encapsulated complex can not exit the zeolite.

Characterization of the Modified Zeolite

The final $[Cu^{II}L]_nY$ samples obtained after the ion-exchange encapsulation process were characterized by surface analysis (XRD, SEM and XPS), spectroscopic methods (FTIR and EPR), chemical analysis (CA) and thermal analysis (TGA).

Powder X-ray diffraction patterns of the $[Cu^{II}L]_nY$ samples and the parent NaY are very similar. The unit-cell parameters were calculated from the (5 3 3), (6 4 2) and (5 5 5) reflection peak positions which were determined using the (1 1 1) reflection of the quartz (2θ = 26.64187) as an internal standard by ASTM D 3942–80. No variation was observed in the zeolite lattice parameters after the encapsulation process. This result shows that no significant structural changes in the zeolite framework occur (i.e., crystallinity of NaY is preserved) during the encapsulation process and that the zeolite structure is retained upon metal-complex encapsulation. Peaks due to the neat complex were not detected, probably because of its very low percentage loading.

$[Cu^{II}L]_nY$ samples obtained after the ion-exchange encapsulation process were analyzed by SEM. Analysis of the SEM micrographs of the parent and modified samples indicates that there were no changes in the NaY morphology and structure upon complex encapsulation (Figure 1). Furthermore, the SEM results confirm that Soxhlet extraction is a suitable method for removing all the uncomplexed ligand and the residual metal complex physically adsorbed on the external surface of zeolite.

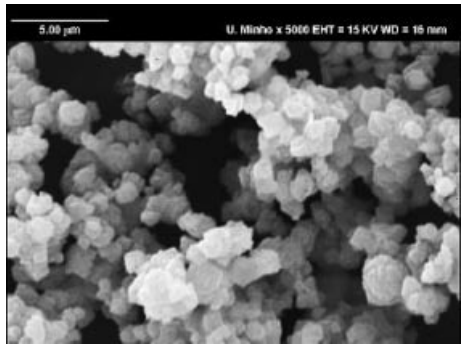

Figure 1. Scanning electron micrograph of $[Cu^{II}L]_{10}Y$ after Soxhlet extraction.

The infrared spectra of the parent NaY (**A**), $[Cu^{II}L]_7Y$ (**B**) and purine ligand (**C**) are presented in Figure 2. As the FTIR spectroscopic patterns of the $[Cu^{II}L]_nY$ samples prepared at different pH values were very similar, the sample $[Cu^{II}L]_7Y$ was chosen as a representative example.

The spectra of the parent zeolite and $[Cu^{II}L]_7Y$ are dominated by the strong bands attributable to the zeolite structure. No shift or broadening of the zeolite vibration bands are observed upon inclusion of the complex, which provides further evidence that the zeolite structure remains unchanged after the encapsulation procedure. In the $[Cu^{II}L]_7Y$ spectrum, the presence of the encapsulated organic complexes can be detected by small bands at $\tilde{\nu}_{max}$ = 1503, 1465 and 1395 cm^{-1}, typical of the purine ring, which appear shifted relative to those of the free ligand. The absence of N–H stretching vibration at $\tilde{\nu}_{max}$ = 3273 cm^{-1} is evidence of the copper-ion coordination with the purine

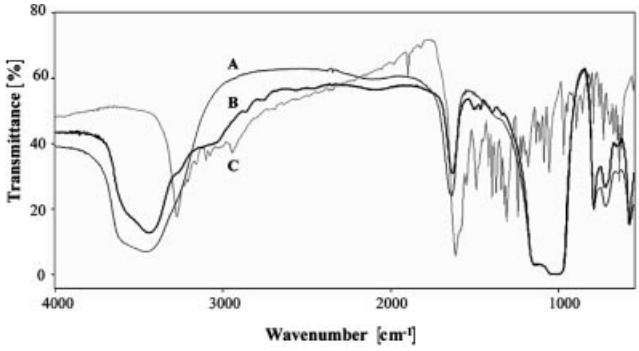

Figure 2. FTIR spectra of (A) NaY, (B) $[Cu^{II}L]_7Y$ and (C) purine ligand.

ligand and of the absence of free ligand within the zeolitic matrix. The obtained FTIR spectroscopic data indicate that the metal complex has been encapsulated in the Y zeolite and also suggest the presence of host–guest interactions with the zeolite structure.

Chemical analyses were also carried out on the solid $[Cu^{II}L]_nY$ samples. The obtained results, together with the molar Si/Al ratio and the estimated number of copper ions per unit cell, are presented in Table 2.

Table 2. Chemical analysis of the solid $[Cu^{II}L]_nY$ samples.

	Elemental analysis [wt.-%]						Cu/C	Cu/N
	Si/Al	Cu^{II} [a]	Cu^{II}/UC	C	H	N	(w/w)	(w/w)
NaY	2.88	–	–	–	–	–	–	–
$[Cu^{II}L]_{5.4}Y$	2.95	0.43	1.10	1.70	3.20	1.50	0.25	0.28
$[Cu^{II}L]_7Y$	2.98	0.32[b]	0.76[b]	1.00	3.00	0.90	0.32	0.35
$[Cu^{II}L]_{10}Y$	2.93	0.41	0.96	1.30	2.90	1.10	0.32	0.37

[a] Copper loading on NaY. [b] Copper loading after the $NaNO_3$ treatment on NaY.

Table 2 shows that the maximum of one metal ion per unit cell is obtained on the $[Cu^{II}L]_{5.4}Y$ sample. It can also be calculated that the $(AlO_4)^-$ charges in the modified samples are not fully compensated by Cu^{2+} and Na^+ ions. Most likely, protons balance the remaining charges through the following reaction taking place in aqueous solution:

$$\text{purine(aq)} + Cu^{2+}(aq) + H^+(aq) + Na^+(Z) \rightarrow Cu[\text{purine}]_n(Z) + Na^+(aq) + H^+(Z)$$

Charge compensation by co-exchange of protons led to some residual acidity in the zeolite, even in the samples for which NaOH was used to adjust the pH value during the preparation procedure. This residual acidity could have an effect on the catalytic behaviour of the samples in the cyclohexene oxidation reaction.[8]

The molar Si/Al ratio in $[Cu^{II}L]_nY$ samples did not change substantially upon Cu^{II} complex exchange, indicating that dealumination does not occur during the encapsulation procedure. The comparisons of the molar Si/Al ratios for NaY and the modified samples confirm that the preparation method used in this work does not modify the zeolite structure, in agreement with XRD and FTIR results.

The success of the encapsulation of Cu^{II}–purine complexes in NaY was confirmed by the analytical data of carbon and nitrogen obtained by elemental analysis and by the copper loading obtained by ICP-AES (Table 2). The results suggest the presence of different structures of Cu^{II}–purine complexes with preferential Cu/ligand stoichiometry of 1:2 and 1:3.

For the 9-methyl-6-(methylamino)purine ligand, with a cation pK_a value equal to 4.2,[18] the ratio of ligand·H^+/ligand observed at different pH syntheses is 5×10^{-2} for pH = 5.4, 1.3×10^{-3} for pH = 7.0 and 1.3×10^{-7} for pH = 10.0. In acidic media, the purine ring can be protonated at N^1 (the more basic centre in the purine ring). This protonation hinders the coordination of the purine-ring nitrogen atoms (N^1 and N^7) with the copper ion; the formation of complexes such as **g** and **h** (Scheme 1) may be then favoured. In neutral medium, complex **h** is mainly present with two purine ligands that coordinate through the nitrogen atoms (NNNN) around the copper ion.[19,20] In more basic solutions, the nitrogen atoms of the purine ring are activated to coordinate with the copper ion, and complex **c** may be formed.

The XPS technique, which allows an analysis of the inner structure and cavity contents up to a depth of about 50 Å,[21] can provide information about the presence and distribution of Cu^{II}–purine complexes through the surface layer of NaY as well as on the oxidation state of the metal. All samples revealed the presence of oxygen, silicon and aluminium in their XPS resolution spectra. In the $[Cu^{II}L]_nY$ samples, the presence of the copper and nitrogen from the metal complexes was detected. In the Cu $2p_{3/2}$ and N 1s region, bands typical of the Cu^{II} complexes, scarcely intense because of their low loading (as confirmed by XRD analyses), were identified. Table 3 presents the surface atomic content of sodium, silicon, aluminium and copper, obtained from the area of the relevant bands in the XPS spectrum for $[Cu^{II}L]_nY$ samples.

Table 3. Areas under the XPS Al 2p, Si 2p, Na 1s, C 1s, N 1s and Cu 2p bands for the samples.

	XPS [atom-%]				
	Si	Al	Na	Cu^{II}	Si/Al
NaY	23.8	7.4	11.4	–	3.10
$[Cu^{II}]Y$	23.5	7.6	8.5	0.30	2.98
$[Cu^{II}L]_{5.4}Y$	25.1	5.6	3.3	0.10	4.32
$[Cu^{II}L]_7Y$	22.4	7.1	7.0	0.50	3.03
$[Cu^{II}L]_{10}Y$	22.1	7.3	8.6	0.40	2.92

The increase in the Si/Al ratio in the modified $[Cu^{II}L]_{5.4}Y$ sample suggests that a certain dealumination takes place at the surface of the material during the encapsulation process in this case.

For $[Cu^{II}L]_7Y$ and $[Cu^{II}L]_{10}Y$ samples, the amount of Cu from XPS is very similar to the bulk copper content (Table 2). Probably, the Cu^{II}–purine complexes are homogeneously distributed throughout the NaY structure. However, for $[Cu^{II}L]_{5.4}Y$ the metal complexes diffuse through NaY and are preferentially located within the inner cavities.

A medium binding-energy value of 932.2 eV for Cu $2p_{3/2}$ is obtained from the XPS spectra of $[Cu^{II}L]_nY$ samples, which confirms that the metal is in a +2 oxidation state, in agreement with the copper coordination sphere of the free complex. The same oxidation state is observed for the $[Cu^{II}]Y$ sample. All samples exhibit N 1s as a band centred at 400 eV, due to the contribution of the amine nitrogen atom of the 9-methyl-6-(methylamino)purine ligand. This result shows that the host matrix environment does not affect the valence state of the metal atom of the complexes.

Powder EPR spectra of all $[Cu^{II}L]_nY$ samples obtained at room temperature are typical of magnetically diluted samples, implying that the Cu^{II}–purine complexes are dispersed within the supercages of NaY, which acts as a diamagnetic matrix. The corresponding $g_{\|}$ and $A_{\|}$ values, summarized in Table 4, are axial type and exhibit well-resolved hyperfine couplings with copper ($^{63}Cu/^{65}Cu$, $I = 3/2$) in the region of low magnetic fields.[9,10]

Table 4. EPR data of the solid $[Cu^{II}L]_nY$ samples.

Sample	$g_{\|}$	$g_{\perp}$	$A_{\|}$ / 10^{-4} cm^{-1}
$[Cu^{II}L]_{5.4}Y$	2.490	2.045	150
$[Cu^{II}L]_{7}Y$	2.309	2.049	180
$[Cu^{II}L]_{10}Y$	2.302	2.047	175

EPR spectra of the samples prepared at pH = 7.0 and pH = 10.0 (Figure 3) show g and A values typical of planar coordination of nitrogen and/or oxygen in the first coordination sphere around Cu^{II}.[8,9,16,19] In contrast, the EPR spectrum of the $[Cu^{II}L]_{5.4}Y$ sample is complex, probably because of the presence of more than one complex species. The increase in $A_{\|}$ and the decrease in $g_{\|}$ values (see Table 4) suggest an NNNN coordination around the Cu^{2+} ion.[20,22–24]

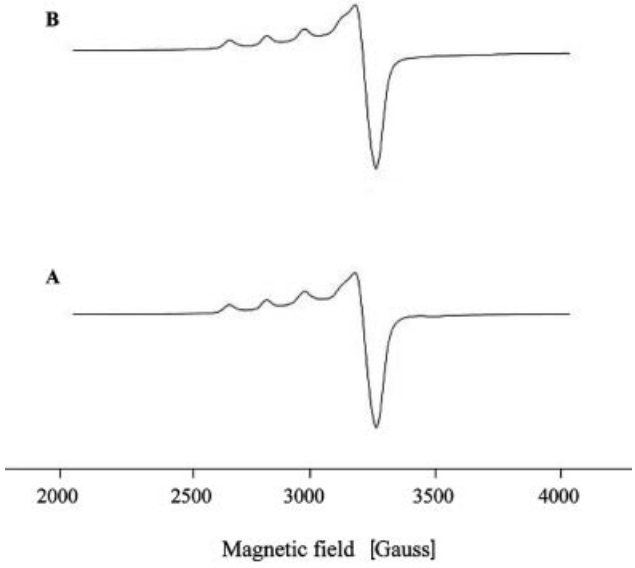

Figure 3. EPR spectra of (A) $[Cu^{II}L]_7Y$ and (B) $[Cu^{II}L]_{10}Y$.

In agreement with Weckhuysen et al. who reported two different coordination modes of the Cu^{II}–histidine complexes encapsulated in NaY zeolite,[6–10,20] three different Cu^{II}–purine complexes are proposed for inside the zeolitic supercage: (i) complexes **A** and **B** with a 1:2 Cu/L stoichiometry and (ii) complex **C** with a 1:3 Cu/L stoichiometry. As shown in Scheme 2, Cu^{II} is coordinated with the 9-methyl-6-(methylamino)purine ligands in complex **A** by means of two $N_{am}N^7$ chelating groups [with an $N_{am}(1)N^7(1)$-$N_{am}(2)N^7(2)$ coordination, where the numbers in brackets refer to the 9-methyl-6-(methylamino)purine molecule], while complex **B** is characterized by an $N_{am}(1)N_{am}(2)O_wO_z$ coordination, in which O_w and O_z symbolize a water and a zeolite framework oxygen, respectively. An $N_{am}(1)N_{am}(2)$-$N_{am}(3)O_z$ coordination is finally observed for complex **C**.

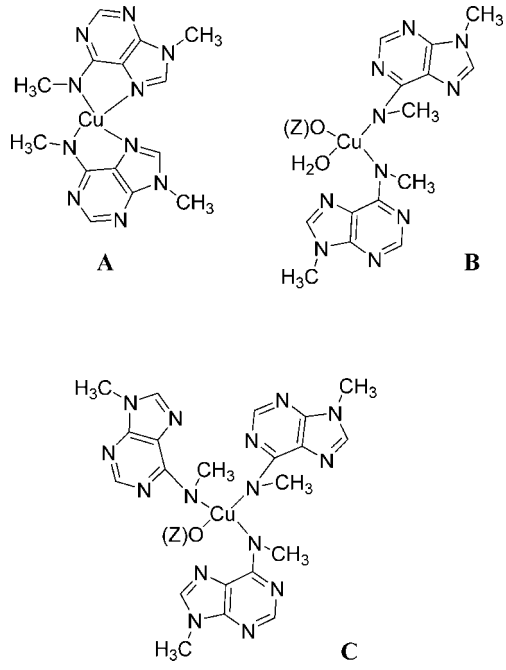

Scheme 2. Structures of copper(II)–purine complexes in Y zeolite: complex **A** with $N_{am}(1)N^7(1)N_{am}(2)N^7(2)$ coordination; complex **B** with $N_{am}(1)N_{am}(2)O_zO_w$ coordination; complex **C** with $N_{am}(1)$-$N_{am}(2)N_{am}(3)O_z$ coordination.

Although complex **A** is the dominant configuration for all samples, the relative amount of the different structures depends on the preparation conditions of the samples. It seems that the pH value during the synthesis determines the mode of coordination of the Cu^{II} ion with the purine ligand; higher values (pH = 7.0 and 10.0) foster the formation of complex **A**, which accounts for 80% in both cases, while at lower pH (5.4) an increase in the amount of complexes **B** and **C** was observed.

Complementary studies performed by using thermal analysis (TGA) contributed to a better understanding of the different configurations of the encapsulated metal (depending on the pH value during the synthesis) on the thermal properties of the samples. The TGA curve of NaY shows a weight loss at 120 °C which can be attributed to the removal of intrazeolite water. After encapsulation of Cu^{II}–purine complexes, two major stages of weight loss can be found in a broad temperature range (i.e., 110–490 °C). The first stage occurs above 110 °C with comparable weight

losses for the three $[Cu^{II}L]_nY$ samples, and it is most likely caused by intrazeolite water desorption and by desorption of water associated with the encapsulated complexes. However, differences were observed at higher temperatures in the second stage of the TGA curves, which corresponds to the decomposition of the encapsulated complexes, both in the onset temperature of the decomposition process and in the weight-loss extent. Results are summarized in Table 5.

Table 5. Thermogravimetric analysis results of the solid $[Cu^{II}L]_nY$ samples.

Sample	T_1[a] [°C]	T_2[b] [°C]	Weight loss[c] [%]
NaY	120	–	–
$[Cu^{II}L]_{5.4}Y$	110	350	5.4
$[Cu^{II}L]_7Y$	110	420	3.2
$[Cu^{II}L]_{10}Y$	110	480	3.7

[a] Temperature of water desorption obtained from DTG curve. [b] Temperature of complex decomposition obtained from DTG curve. [c] Weight loss due to complex decomposition obtained from DTG curve.

Differences in weight losses and onset temperatures of the complex decomposition are most probably related to (i) different coordination configurations of the Cu^{II} ion with the 9-methyl-6-(methylamino)purine ligand which leads to three Cu^{II}–purine complexes, in agreement with chemical analysis and EPR results, and (ii) predominance of one of these Cu^{II}–purine complexes for high pH syntheses.

Catalytic Behaviour of the Modified Zeolite

The effect of Cu^{II}–purine complexes encapsulated in NaY zeolite on the oxidation of cyclohexene with *t*BuOOH (TBHP) in decane was studied, and the results are shown in Table 6.

Table 6. Catalytic performance of the $[Cu^{II}L]_nY$ samples in cyclohexene oxidation.[a]

Catalyst	Conversion[a]	Selectivity [%]		
	[%]	Ketone[b]	Alcohol[c]	Oxide[d]
–	40.3	62.7	37.3	0.0
NaY	40.8	59.0	41.0	0.0
$[Cu^{II}]Y$	46.4	65.9	34.1	0.0
$[Cu^{II}L]_{5.4}Y$	47.6	49.3	42.4	8.3
$[Cu^{II}L]_7Y$	55.8	48.4	37.0	14.6
$[Cu^{II}L]_{10}Y$	65.9	48.9	41.3	9.8

[a] In decane, 30 °C, TBHP/cyclohexene molar ratio = 5:3. [b] 2-Cyclohexene-1-one. [c] 2-Cyclohexene-1-ol. [d] Cyclohexene oxide.

Cyclohexene conversion and product selectivity were compared at 24 hours on-stream. Blank runs were performed to check the contribution of the radical mechanism; it was found that it accounted for about 40% of cyclohexene conversion. Only allylic oxidation occurred with the formation of 2-cyclohexene-1-one, 2-cyclohexene-1-ol and 3-*tert*-butylcyclohexenyl peroxide, as also reported in ref.,[25] while the formation of cyclohexene oxide was not observed. The NaY sample showed a quite similar behaviour.

When sodium was ion-exchanged with copper in NaY ($[Cu^{II}]Y$), a slight increase was observed both in conversion and in 2-cyclohexene-1-one selectivity. The increase in conversion from 46.4% to 65.9%, which is found by comparing the $[Cu^{II}]Y$ and $[Cu^{II}L]_{10}Y$ samples, indicates that in the presence of the purine ligand the catalytic activity is increased by a factor of 1.42. From the results in Table 6, it is evident that 2-cyclohexene-1-one is selectively formed in the presence of all catalysts. However, cyclohexene oxide is formed only on the $[Cu^{II}L]_nY$ catalysts, when Cu^{II} is coordinated to the purine ligands. The selectivity value towards the epoxide seems to have a slight maximum for the $[Cu^{II}L]_7Y$ sample, while conversion increases continuously with the pH value used during the catalyst preparation. The 2-cyclohexene-1-ol selectivity also shows an increase for all the $[Cu^{II}L]_nY$ catalysts with respect to the $[Cu^{II}]Y$ sample. Further, in agreement with the findings of other authors,[7,25] the presence of 1,2-cyclohexanediol was not observed.

The formation of the allylic oxidation products, 2-cyclohexene-1-one and 2-cyclohexene-1-ol, suggests the preferential attack of the activated C–H bond over the C=C bond. Furthermore, the formation of 3-*tert*-butylcyclohexenyl peroxide is an indication of the occurrence of radical reactions.[25–28] TBHP as the oxidant promotes the allylic oxidation pathway and the extent of epoxidation is reduced. The effect of molecular oxygen in the cyclohexene epoxidation reaction with *t*BuOOH has also been reported.[29,30] It was found that when molecular oxygen acts as an oxidant in the reaction, 2-cyclohexene-1-one and 2-cyclohexene-1-ol are mainly formed.

Conclusions

In light of the obtained results, it can be concluded that Cu^{II}–purine complexes coordinated with a 9-methyl-6-(methylamino)purine ligand can be encapsulated in NaY zeolite by an ion-exchange adsorption process, without structural modification or loss of crystallinity of the zeolite framework. Depending on the pH of the exchange solution, three different structures for the Cu^{II}–purine complexes have been proposed in the Y zeolite supercage: (i) complex **A** is located in the centre of the supercage, for which all equatorial coordination sites are provided by the purine molecules; (ii) complex **B** is coordinated to two purine molecules, for which the other two ligands are supplied by the zeolite and a water molecule; and (iii) complex **C** is coordinated to three purine ligands and to one framework oxygen atom from the zeolite.

$[Cu^{II}L]_nY$ catalysts are active in the cyclohexene oxidation reaction with TBHP. The product distribution is mainly consistent with the allylic oxidation to 2-cyclohexene-1-one and 2-cyclohexene-1-ol.

Experimental Section

Materials: NaY zeolite (Si/Al = 2.88) was supplied by Grace GmbH. Chemicals for the purine ligand synthesis, the encapsulation procedure [EtOH, NaOH, HCl, $Cu(NO_3)_2{\cdot}3H_2O$ and

$NaNO_3$] and the oxidation reaction (cyclohexene, decane, *t*BuOOH [70% solution in water]) were purchased from Aldrich. All used materials were reagent grade.

Sample Preparation: The 9-methyl-6-(methylamino)purine ligand was synthesized as described in detail elsewhere.[31] Zeolite-encapsulated Cu^{II}–purine complexes were prepared according to the following experimental procedure: aqueous solutions of $Cu(NO_3)_2 \cdot 3H_2O$ (8.5 mg, 3.52×10^{-2} mmol) and the 9-methyl-6-(methylamino)purine ligand (29.0 mg, 1.76×10^{-1} mmol) in distilled water (100 cm^3) (purine/Cu^{II} = 5:1; this molar ratio ensures that the purine ligand is not the limiting reactant during the encapsulation process) were added to NaY (0.5 g; previously calcined at 500 °C during 8 h under a dry air stream) at different pH (5.4, 7.0 and 10.0). Aqueous solutions of NaOH and/or HCl (0.1 mol dm^{-3}) were used to adjust the pH value, which was continuously monitored. The resulting mixtures were stirred at room temp. for 24 h, until the brown-green aqueous solutions became colourless, indicating that the complex was adsorbed by the zeolite. Then the suspension was filtered off, and the solid was washed with distilled water and dried at 60 °C for 8 h. The excess or uncoordinated ligand, as well as the residual metal complex physically adsorbed on the external surface, was removed by Soxhlet extraction with ethanol for 6 h. Finally, the samples were dried in an oven at 100 °C, under vacuum, for 12 h. The obtained samples are denoted as $[Cu^{II}L]_nY$, where L represents the 9-methyl-6-(methylamino)purine ligand and *n* is the pH value. A $[Cu^{II}]Y$ sample, with the same amount of copper as $[Cu^{II}L]_nY$, was also prepared for comparison. A portion of the $[Cu^{II}L]_7Y$ sample was further treated, for 6 h at room temp., with an aqueous solution of $NaNO_3$ (0.1 mol dm^{-3}) in order to remove the remaining uncomplexed copper ions from the zeolite; it was subsequently filtered off, washed with hot distilled water and finally dried at 60 °C for 12 h.

Characterization: Elemental chemical analyses (Si, Al, Na and Cu) were performed by inductively coupled plasma atomic emission spectrometry (ICP-AES) using a Philips ICP PU 7000 Spectrometer. The decomposition of solid samples was carried out by alkaline fusion; the method involves the use of lithium metaborate as the fluxing agent, which grants thermal stabilization of elements during the fusion stage at 1050 °C.[15] Chemical analysis of C, H and N were carried out with a Leco CHNS-932 analyzer. X-ray photoelectron spectroscopy analyses were obtained at the C. A. C. T. I. (Vigo University, Spain) with a VG Scientific ESCALAB 250iXL spectrometer using monochromatic Al-K_α radiation (1486.92 eV). Powder EPR spectra were obtained with a Bruker EMX spectrometer working at the X-band microwave frequencies (ca. 9.5 GHz) at room temp. Phase analysis was performed by XRD using a Philips PW1710 diffractometer. Scans were taken at room temp. in a 2θ range between 4 and 80°, using Cu-K_α radiation. The SEM micrographs were collected with a LEICA Cambridge S360 Scanning Microscope equipped with an EDS system. To avoid the surface charging, samples were coated with gold in vacuo, by using a Fisons Instruments SC502 sputter coater, before being observed. Room temp. FTIR spectra of ligand and sample materials were obtained from powdered samples on KBr pellets, using a Bomem MB104 spectrometer in the range 4000–500 cm^{-1} by averaging 20 scans at a maximum resolution of 4 cm^{-1}. The electronic UV/Vis absorption spectra of the purine ligand and residual solutions were collected in the range 600–200 nm with a Shimadzu UV/2501PC spectrophotometer using quartz cells at room temp. Thermogravimetric analyses (TGA) of the samples were carried out using a TGA 50 Shimadzu instrument under a high-purity helium flow (50 $cm^3 min^{-1}$). All samples were characterized between 25 and 600 °C with a heating rate of 6 °C min^{-1}.

Catalytic Runs

Experimental runs lasting 24 h were performed in a magnetically agitated batch reactor, equipped with an external water jacket and with a refrigerant, each connected with a cryothermostat in order to control the reaction and condensation temperatures, respectively. Prior to the catalytic tests, samples were activated in an oven at 250 °C for 2 h. The reaction conditions were T = 30 °C, catalyst: 30 mg, cyclohexene: 100 μL, *t*BuOOH (5.5 mol dm^{-3} in decane): 945 μL, oxidant/substrate molar ratio = 5:3 and solvent: decane.

Chromatographic analyses of the reaction mixture, sampled at 1-h intervals, were carried out using a GC HP 6890 (equipped with a capillary column SUPELCO Petrocol DH and a FID) and allowed qualitative and quantitative determination of (by the internal standard method) the reactant, cyclohexene and the following reaction products: cyclohexene oxide, 2-cyclohexene-1-one, 2-cyclohexene-1-ol and 1,2-cyclohexanediol. Other products were also observed (but not quantified) and identified by GC-MS: 3-*tert*-butylcyclohexenyl peroxide and very small amounts of 2,3-epoxycyclohexanone and 2,3-epoxycyclohexanol, together with those derived from the thermal decomposition of the *t*BuOOH.

Acknowledgments

Dr. C. S. Rodriguez (C. A. C. T. I., Vigo University, Spain) is gratefully acknowledged for performing and interpreting the XPS analyses. Acknowledgments are also due to Dr. C. L. Remesar (GIQIMO, Santiago de Compostela University, Spain) for the EPR measurements. We thank Dr. A. S. Azevedo for collecting the powder diffraction data and Dr. C. Ribeiro for performing chemical analyses (Departamento de Ciências da Terra of Universidade do Minho). This work was supported by the Centro de Química (University of Minho, Portugal) and by Fundação para a Ciência e Tecnologia (FCT Portugal), under programme POCTI-SFA-3-686.

[1] P. P. Knops-Gerrits, D. E. De Vos, F. Thibault-Starzyk, P. A. Jacobs, *Nature* **1994**, *369*, 543–546.
[2] D. E. De Vos, P. P. Knops-Gerrits, R. F. Parton, B. M. Weckhuysen, P. A. Jacobs, R. A. Schoonheydt, *J. Inclusion Phenom. Mol. Recognit. Chem.* **1995**, *21*, 185–213.
[3] A. Corma, H. Garcia, *Eur. J. Inorg. Chem.* **2004**, 1143–1164.
[4] H. Arakawa, M. Aresta, J. N. Armor, M. A. Barteau, E. J. Beckman, A. T. Bell, J. E. Bercaw, C. Creutz, E. Dinjus, D. A. Dixon, K. Domen, D. L. DuBois, J. Eckert, E. Fujita, D. H. Gibson, W. A. Goddard, D. W. Goodman, J. Keller, G. J. Kubas, H. H. Kung, J. E. Lyons, L. E. Manzer, T. J. Marks, K. Morokuma, K. M. Nicholas, R. Periana, L. Que, J. Rostrup-Nielson, W. M. H. Sachtler, L. D. Schmidt, A. Sen, G. A. Somorjai, P. C. Stair, B. R. Stults, W. Tumas, *Chem. Rev.* **2001**, *101*, 953–996.
[5] T. Katsuki, *Coord. Chem. Rev.* **1995**, *140*, 189–214.
[6] B. M. Weckhuysen, A. A. Verberckmoes, I. P. Vannijvel, J. A. Pelgrins, P. L. Buskens, P. A. Jacobs, R. A. Schoonheydt, *Angew. Chem. Int. Ed. Engl.* **1996**, *34*, 2652–2654.
[7] B. M. Weckhuysen, A. A. Verberckmoes, L. Fu, R. A. Schoonheydt, *J. Phys. Chem.* **1996**, *100*, 9456–9461.
[8] B. M. Weckhuysen, H. Leeman, R. A. Schoonheydt, *Phys. Chem. Chem. Phys.* **1999**, *1*, 2875–2880.
[9] R. Grommen, P. Manikandan, Y. Gao, T. Shane, J. J. Shane, R. A. Schoonheydt, B. M. Weckhuysen, D. Goldfarb, *J. Am. Chem. Soc.* **2000**, *122*, 11488–11496 and references therein.
[10] D. Baute, D. Arieli, F. Neese, H. Zimmermann, B. M. Weckhuysen, D. Goldfarb, *J. Am. Chem. Soc.* **2004**, *126*, 11733–11745.
[11] G. Sienel, R. Rieth, K. T. Rowbottom, *Ulmann's Encyclopedia of Industrial Chemistry*, 7th ed., Wiley-VCH, **2004**, vol. A9, p. 531–545.

[12] J. H. Lister, *Chemistry of Heterocyclic Compounds*, Wiley-Interscience, New York, **1971**, vol. 24 (II).
[13] G. Shaw, *Comprehensive Heterocyclic Chemistry I* (Eds.: K. T. Potts), Pergamon Press, Oxford, **1984**, vol. 5.
[14] J. B. Lambert, H. F. Shurvell, D. A. Lightner, R. G. Cooks, *Organic Structural Spectroscopy*, Prentice-Hall, New Jersey, **1998**.
[15] N. Nunes, F. Costa, A. M. Fonseca, I. C. Neves, M. A. Carvalho, C. Ribeiro, *Mater. Sci. Forum* **2006**, *514–516*, 1246–1249.
[16] I. Neves, C. Freire, A. N. Zakharov, B. Castro, J. L. Figueiredo, *Colloids Surf., A* **1996**, *115*, 249–256.
[17] F. Costa, C. J. R. Silva, M. M. M. Raposo, A. M. Fonseca, I. C. Neves, A. P. Carvalho, J. Pires, *Microporous Mesoporous Mater.* **2004**, *72*, 111–118.
[18] D. J. Brown, N. W. Jacobsen, *J. Chem. Soc.* **1965**, 3770–3778.
[19] J. G. Mesu, T. Visser, F. Soulimani, E. E. van Faassen, P. de Peinder, A. M. Beale, B. M. Weckhuysen, *Inorg. Chem.* **2006**, *45*, 1960–1971.
[20] J. G. Mesu, T. Visser, A. M. Beale, F. Soulimani, B. M. Weckhuysen, *Chem. Eur. J.* **2006**, *12*, 7167–7177.
[21] J. C. Vendrine, *Catalyst Characterization. Physical Techniques for Solid Materials* (Eds.: B. Imelik, J. C. Vendrine), Plenum Press, New York, **1994**, p. 467.
[22] H. J. Scholl, J. Hutermann, *J. Phys. Chem.* **1992**, *96*, 9684–9691.
[23] R. Lontie, *Copper Proteins and Copper Enzymes*, CRC Press, Boca Raton, FL, **1984**, vols. 1–3.
[24] A. Neves, C. N. Verani, M. A. Brito, I. Vencato, A. Mangrich, G. Oliva, D. D. H. F. Souza, A. A. Batista, *Inorg. Chim. Acta* **1999**, *290*, 207–212.
[25] M. Salavati-Niasari, M. Hassani-Kabutarkhani, F. Davar, *Catal. Commun.* **2006**, *7*, 955–962.
[26] J. D. Koola, J. K. Kochi, *J. Org. Chem.* **1987**, *52*, 4545–4553.
[27] R. A. Sheldon, J. K. Kochi, *Adv. Catal.* **1976**, *25*, 272–413.
[28] S. V. Kotov, S. Boneva, T. Kolev, *J. Mol. Catal. A* **2000**, *154*, 121–129.
[29] T. G. Carrell, S. Cohen, G. C. Dismukes, *J. Mol. Catal. A* **2002**, *187*, 3–15.
[30] P. Forzatti, F. Trifirò, *React. Kinet. Catal. Lett.* **1974**, *1*, 367–372.
[31] R. K. Robins, H. H. Lin, *J. Am. Chem. Soc.* **1957**, *79*, 490–494.
Received: November 3, 2006
Published Online: March 13, 2007

